1

Materials for 3D Printing

Thomas McDonagh, Bin Zhang and Sheng Qi

School of Pharmacy, University of East Anglia, Norwich, UK

1.1 Introduction

Three-dimensional printing (3DP), also known as Additive Manufacturing (AM), has emerged as an exciting technology for the manufacture of pharmaceutical products for personalised patient treatment. The interindividual variability of the human population is a constant challenge when striving for effective drug delivery because patients come in different shapes, sizes, ages, genetics, and necessities and so require medication personalised to their needs for the most effective outcomes [1, 2]. 3DP has been shown to be a flexible technique that can be used to manufacture drug delivery devices (DDDs) for a wide array of applications such as tablets, implants, microneedles, and suppositories [3–5]. In addition, compared to conventional large-scale production techniques such as tablet pressing, 3DP is much more flexible with the potential to simplify supply chains and accelerate development cycles. Such traits make 3DP an ideal candidate technology to produce on-demand personalised medicines and in turn improve patient quality of life. However, there are still several challenges hindering its adoption. Limited availability of biocompatible materials, the incompatibility of the active pharmaceutical ingredient) (API), and/or polymer with the printing conditions, and regulatory hurdles present a significant challenge when designing 3DP pharmaceutical products. This is highlighted by the presence of just one 3DP pharmaceutical product currently on the market as of 2023, Spritam® [6].

3D Printing of Pharmaceutical and Drug Delivery Devices: Progress from Bench to Bedside, First Edition.
Edited by Dimitrios A. Lamprou, Dennis Douroumis and Sheng Qi.

Material choice is a fundamental consideration when designing a pharmaceutical dosage form. All drug products are comprised of an API (the bioactive component) and inactive functional excipients which facilitate the release of the API to the target location in the body. With the advance of 3D-printing medicine, API carrier materials have an increasingly important role in not only protecting the API in a convenient printable package and disguising unpalatable ingredients but also in facilitating complex release profiles. Several 3D-printing techniques are applicable for manufacturing DDD: Thermal Extrusion-based deposition systems (TE); Semi-solid extrusion (SSE); Stereolithography (SLA); and Powder Bed fusion (PBF). Successful printing of pharmaceuticals requires consideration of the nature of the 3D-printing process. Each technique has its own benefits and limitations in terms of material compatibility, print quality, and scalability and so must be considered as a whole when designing a new DDD. The objective of this chapter is to first discuss each printing technique, exploring the key material characteristics and processing parameters that influence both printability and drug delivery performance. Subsequently, the materials which have shown suitability for 3DP manufacture of DDD will be discussed with a focus on the key material attributes relevant for printing and drug release properties.

1.2 Material Processability Considerations for Pharmaceutical 3DP

1.2.1 Thermal Extrusion-Based 3D Printing

Thermal extrusion (TE)-based 3D printing is a popular solvent free 3DP technique for printing thermoplastic polymer and API formulations. In TE printing, thermal energy is applied to a print head to melt material, enabling extrusion through a nozzle onto a build plate. Thermoplastic polymers are used because they are composed of long linear chains, held together by weak attraction forces. When subjected to high temperatures in the print head, they soften or melt to enable extrusion before solidifying upon cooling. The nozzle and/or build plate are controlled by linear actuators that enable precise deposition into a pre-defined geometry in a layer-by-layer fashion according to a 3D digital model. Good print resolution is achievable with resolutions typically between 100 μm and 400 μm [7, 8], depending on the diameter of nozzle used. A benefit of TE printing is the minimal post processing requirements. Printed parts are full strength immediately after printing and unlike other 3DP techniques, no washing or drying steps are required. Furthermore, release rates of TE drug products are highly tuneable by varying printing software parameters such as infill density [9]. Due to the mechanical stability of TE drug products, this technique appears to be more suitable for controlled or sustained release applications [10, 11], although immediate release pharmaceutical products have also been explored [12].

Most current TE 3DP technologies are not compatible with the direct printing of raw powder materials. Direct TE of powders presents challenges in terms of feeding (poor flowability), homogenous mixing, and degassing (trapped air between powder particles) [13]. As such, a prior hot-melt extrusion (HME) step is commonly used to sufficiently mix reagents and process them into a more attractive feedstock for printing. In HME, heat and mechanical shear is used to mix reagents producing a homogenous melt which can be extruded into uniform filaments. Most pharmaceutical polymers require a temperature of at least 15 °C to 60 °C above their glass transition (T_g) to be sufficiently molten for processing [14]. Filaments can be printed using the widespread, low-cost technology fused deposition modelling (FDM) or can be pelletised into granules for use with direct granule TE.

1.2.1.1 Thermal Considerations

The first material processability consideration for TE 3DP concerns the thermal processing. Thermal processing presents a challenge when working with pharmaceutical formulations because some API and polymers are thermolable and will begin to degrade at high temperatures, reducing the efficacy of the pharmaceutical product. Additionally, formulation viscosity is intrinsically linked to temperature. High temperatures increase the kinetics of a formulation, reducing its apparent viscosity [15]. Therefore, successful TE operates within a temperature window that sufficiently reduces the viscosity of the polymer melt (above T_{min}) to enable good mixing and extrusion, whilst maintaining the API stability (below the thermal degradation temperature). To ensure solubility of API in the polymer melt, a third boundary temperature is often introduced, called the solubility line (T_c) [16]. This theoretical design space is shown in Figure 1.1. The design space can be seen to shrink for high drug load formulations due to the increased T_c required to solubilise the API. Additionally, increased residence time in the HME can be used to increase API dissolution but also increases the likelihood of thermal degradation. These same design constraints are also applicable when printing. Lower than optimal printing temperatures increase formulation viscosity that can cause nozzle blockages and low bond strength between printed layers [17] and high temperatures can result in further API degradation and poor print quality.

Whilst some sensitive API may appear to be incompatible with TE due to low thermal degradation temperatures (T_{deg}), strategies exist to reduce the thermal load on formulations enabling printing at lower temperatures. By using these techniques, a wide variety of polymers and API has been successfully printed, with drug loadings from 5% to 60% w/w shown to be feasible [19]. The first technique involves carefully selecting polymers and excipients which are extrudable at low temperatures. This generally involves use of

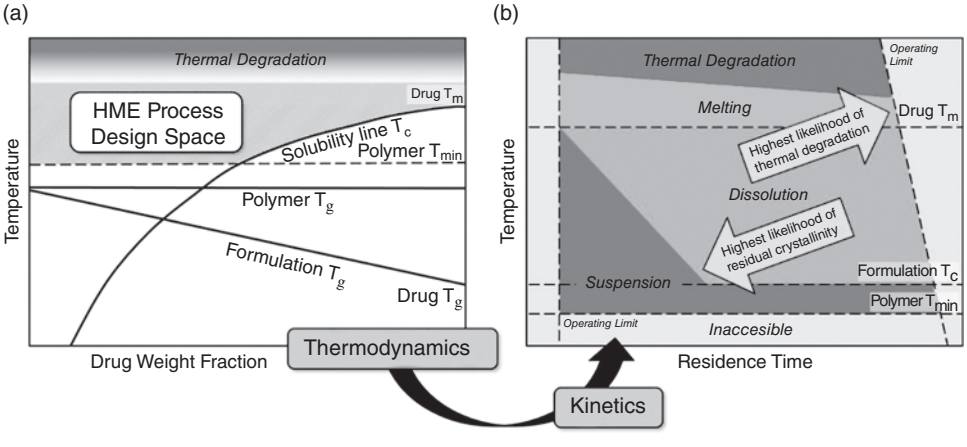

Figure 1.1 *(a) The temperature–composition phase diagram of the hot-melt extrusion process. The temperature design space falls below the thermal degradation temperature and, depending on composition, above the solubility line or polymer's minimum processing temperature T_{min}. Product phase behaviour is governed by the solubility line (formulation T_c) and formulation glass transition T_g. (b) Hot-melt extrusion process operating design space diagram. Three processing regimes (melting, dissolution, and suspension) can be delineated by temperature and kinetic considerations. (Source: Reproduced from [18] with permission from Elsevier 2018.)*

plasticisers which act as a lubricant between segments of polymer chains, thus increasing the materials flexibility and softness. Kollamaram et al. succeeded in printing Ramipril and 4-aminosalicylic acid (4-ASA) loaded tablets using a PVP PVP-VA copolymer system plasticised with PEG 1500 [20]. Ramipril is transformed into the impurity diketopiperazine upon exposure to temperatures higher than its melting point (109 °C) and 4-ASA begins to degrade at 130 °C. Filaments loaded with 3% drug were obtained by HME at 70 °C and tablets were printed at 90 °C. HPLC analysis confirmed that both drugs were stable with no signs of degradation, demonstrating how the careful selection of polymer and plasticiser can enable the printing of thermolabile API at low temperatures. Another technique involves avoiding the thermal and mechanical stress induced during HME altogether by using filament impregnation. The filament impregnation technique was first reported in 2014 [21], where API was loaded into the filament post HME by soaking in a saturated alcoholic drug solution. Whilst several authors have reported on the impregnation technique for DDD applications, drug loading is very low (<3% w/w) [22–24], limiting its use to drugs with therapeutic effects at low dose [25]. Additionally, whilst the impregnation method does avoid the thermal stress induced during HME, the API still has to pass through the heated print head. Goyanes et al. used this method to load 4-ASA into commercially produced Polyvinyl alcohol (PVA) filaments by soaking in a saturated ethanolic drug solution for 24 hours before printing [26]. After printing at 210 °C, the already limited drug loading was reduced by approximately half to 0.12% w/w, indicating that even though residence time in the print head is short (a few seconds) it is sufficient for significant degradation of thermolabile drugs.

1.2.1.2 Solubility Enhancement

One area in which thermal extrusion 3DP coupled with HME has shown great promise is in enhancing the bioavailability of poorly soluble API, opening the door to a host of molecules previously considered unviable as drugs [27]. More than 40% of new chemical entities produced during drug discovery exhibit poor solubility characteristics, greatly limiting their therapeutic effectiveness [28]. API can exist either as a solid suspension or be partially or fully dissolved in the polymer matrix. This crystallinity is highly influence by processing conditions (Figure 1.1). It is desirable that API remain in the amorphous form in DDD so that the dissolution, dispersion, or erosion of the tablets mediate the drug release rather than the solubility of the crystalline drugs. The intense mixing and heating imposed by the rotating screws in HME can cause the API molecules to dissolve in the molten polymer, transforming the crystalline drug into a more uniform, amorphous dispersion. With the drug in an amorphous form, no energy is required to break the drug crystal lattice. For this reason, relative to the crystalline form, the amorphous form of many poorly water-soluble drugs can achieve substantially higher apparent solubility and markedly faster dissolution [29]. For successful results, polymer and functional excipients should be carefully chosen to maximise API solubility. Polymer-API miscibility can be predicated using the Hansen solubility parameter [30]. For poorly miscible formulations, the drug may crystallise out during storage, resulting in physical stability issues and variability in drug release. Sometimes crystallisation inhibitors are added to formulations which can help slow this process [31].

1.2.1.3 Mechanical Considerations

In the case of FDM printing, filament strength and flexibility are a further processing consideration. For successful FDM printing, filaments must possess good mechanical strength

and flexibility to endure the FDM feeding mechanism. This is a significant challenge for DDD applications because most pharmaceutical grade polymers lack such attributes, being either too brittle so that the filaments break in the motor gear or too soft so that they cannot be pushed by the drive gear, thus hindering printing [32, 33]. Recent efforts have been focused on using rheology, filament mechanical screening, and machine learning to identify useful parameters that can be used as predictive tools in pharmaceutical development [34–37]. Xu et al. found toughness to be an effective predictive parameter of filament printability using a simple stiffness test [38]. After screening over 30 in-house manufactured filaments, they found stiffness values greater than 80 g/mm^2 % to be a good indicator of filament printability. When modifying formulations to improve processability, it is important to consider the effects additional excipients will have on the function of the drug product. It is common to incorporate large quantities of additives and plasticisers into the formulation which often do not add any functionality to the main drug delivery and absorption functions, leading to the design of complex formulations with increased weight and increased potential for the adverse stability of the pharmaceutical product. Recently emerging TE techniques, termed direct powder/granule deposition TE, have focused on bypassing the need for filament forming. Using this technique, the HME extrusion and printing steps are effectively combined in a single step printing process. This not only simplifies DDD manufacture but can also be used to print formulations that would not be suitable for forming filaments. Goyanes et al. used a direct single-screw powder extruder (FabRx, UK) to prepare sustained release itraconazole printlets (3D-printed tablets) [39]. McDonagh et al. used a similar granule fed 3DP technology, Arburg Plastic Freeforming (APF), to explore the printability of non-FDM printable formulations [40]. Eudragit E PO, a very brittle polymer loaded with paracetamol, was successfully printed into immediate release tablets without the use of plasticisers. The simplified manufacturing process and more versatile material feed mechanism make direct powder/pellet thermal extrusion an exciting 3DP technology for the future. Table 1.1 summaries the typical polymers used in thermal extrusion 3D printing of solid dosage forms, which are used widely beyond the example studies listed here.

1.2.2 Semi-Solid Extrusion 3DP

Semi-solid extrusion (SSE), also known as pressure-assisted micro syringe (PAM), is a 3DP technique used to print pastes, hydrogels, and other viscous polymer systems. The working principle of SSE is similar to thermal extrusion 3DP in the sense that viscous formulations are extruded through a nozzle to form a 3D structure according to a designed geometry. However, SSE relies on use of a solvent rather than high temperature to obtain the rheological properties to enable extrusion. This allows for much milder printing conditions that enable processing of many biocompatible materials. Khaled et al. state that if a polymer can be processed into powder form, it can be printed using PAM [47]. Room temperature printing is hugely beneficial when working with thermo-sensitive API [4]. However, solvent use also presents challenges in terms of toxicity, API stability, and print quality because a drying step is required post printing that can result in significant shrinkage. SSE printing has shown promise for developing drug eluting tablets [48] and soft scaffolds for tissue engineering [49] and is currently used on the market for printing personalised gummy vitamins [50]. Very high drug loadings up to 96% have been shown to be feasible [51]. Print quality is typically not as good as FDM- and SLA-based printing methods, with resolutions around 200 μm to 400 μm being common [52, 53]. However, high precision drug delivery systems have been shown to be possible with some clever post processing.

Table 1.1 *Examples of polymers used in thermal extrusion 3D printing of pharmaceuticals.*

Polymer	Drug	Printer	Application
Polyvinyl Alcohol (PVA)	Budesonide	MakerBot Replicator 2X Desktop	Controlled release tablets [41]
Hydroxypropyl Methylcellulose (HPMC)	Ibuprofen	MakerBot Replicator 2X Desktop	Controlled release tablets [42]
Polycaprolactone (PCL)	Ibuprofen	Prusa i3 Mk3S	Controlled release tablets [9]
Eudragit® E	Paracetamol	Arburg Plastic Freeformer	Immediate release tablets [40]
Polyurethanes	Dapivirine	Arburg Plastic Freeformer	Controlled release vaginal rings [43]
Hydroxypropylcellulose	Itraconazole	FabRx M3DIMAKER™	Sustained release printlets [39]
Ethylene Vinyl Acetate (EVA)	Indomethacin	MakerBot Replicator 2X Desktop	Intrauterine implant [44]
PLA, PVA, HPMC, HPMCAS, Kollicoat® IR, PEG, Triethyl Citrate	Paracetamol	MakerBot Replicator 2X Desktop	Two pulse, oral drug delivery [45]
PVA, Sorbitol	Lisinopril Dihydrate, Indapamide, Rosuvastatin Calcium and Amlodipine Besylate	MakerBot Replicator 2X Desktop	Polypill [46]

Wu et al. manufactured microneedles patches for glucose delivery using SSE (Figure 1.2d) [54]. Pillar structures were first extruded using a sodium alginate-based paste. Subsequently, the pillars were stretched using a glass cover slide and crosslinked by spraying with a Ca^{2+} solution, producing conical microneedles with tip diameters of 24.5 μm.

1.2.2.1 Rheological Considerations

The materials extruded during SSE printing should be in a semi-solid form, also referred to as a gel or paste. These are formed by mixing polymer(s), functional excipient(s), and the drug with an appropriate solvent at a ratio that results in a paste suitable for printing. As a nozzle-based extrusion technology, optimal pastes should have suitable viscosity, yield stress under shear, compression, and viscoelastic elastic properties [55] to enable continuous printing without blockage. These rheological parameters must also be configured to the geometry of the nozzle in the print head. Depending on nozzle configuration, a wide range of paste viscosities from 30 mPa.s to $>6 \times 10^7$ mPa.s have been reported to be extrudable [56]. Of particular concern to the SSE 3D printing method is the polymer's response to being extruded, how well it is able to adhere to previously printed layers, and its ability to hold the weight of subsequent layers [57]. Shear thinning characteristics are desirable because the viscosity of the paste can be significantly reduced when a high shear rate is exerted during printing. Shear thinning properties influence not only the capability to be pushed through a narrow nozzle at a given temperature but also the ability to regain structure and shape after deposition.

1.2.2.2 Example Applications

First used to produce polypills and tablets, this technology has rapidly evolved to manufacture other types of dosage forms and medical devices. Example applications explored in the literature are chewable tablets, orodispersible films, rectal suppositories, and implantable patches [4]. Some of these applications are shown in Figure 1.2 and Table 1.2. SSE printing has been shown to be a versatile 3DP modality capable of printing a wide range of dosage forms suitable for a variety of release profiles from immediate release tablets to sustained release implants.

1.2.3 Powder Bed Fusion 3D Printing

Powder bed fusion (PBF) 3DP refers to 3D-printing technologies that use powder material as a feedstock. Many polymers and API are available as a powder, making PBF printing a versatile technique for drug delivery device manufacture. Two subset technologies are suitable for pharmaceutical applications: binder jetting (BJ) and selective laser sintering (SLS). Both technologies share the same principle of selectively binding powder in a layer-by-layer fashion to build up a 3D part. In BJ printing, powder binding is achieved by depositing a liquid binder that effectively glues adjacent particles together, whereas in SLS printing, a laser is used to partially melt and agglomerate selected particles. Subsequent layers are built up by spreading a fresh thin layer of powder on top of the bound layer

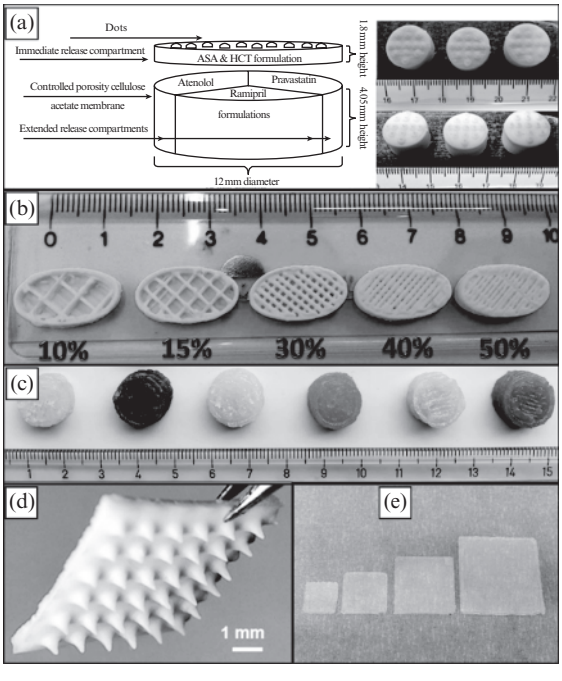

Figure 1.2 *Drug delivery devices manufactured using PAM 3DP. (a) Five-in-one dose Polypill [58]. (b) Floating sustained-release printlets with different fill densities [59]. (c) Chewable isoleucine printlets prepared in different sizes, flavours, and colours [60]. (d) 3D-printed microneedle patch [54]. (e) From left to right: 25, 50, 100, and 200 mm^2 drug loaded films [61]. (Source: Reproduced with permission from [54, 58–61], Elsevier.)*

Table 1.2 *Examples of solid dosage forms and devices produced by SSE 3DP.*

Polymer	Drug	Solvent	Printer	Application
HPMC Poly(Acrylic Acid)	Guaifenesin	Water	Fab@Home, USA	Tablets [57]
Croscarmellose Sodium and Hydroxypropyl Cellulose (HPC)	Levetiracetam (96%)	10% ethanol solution	Desktop semi-solid 3D extrusion printer	Immediate release tablets [51]
HPMC Cellulose Acetate	Nifedipine Captopril Glipizide	Hydro alcoholic Acetone DMSO	RegenHU, Switzerland	Polypill [62]
Cellulose Acetate, D-Mannitol, PEG 6000, Sodium Starch Glycolate, and PVP	Pravastatin (20%), atenolol (30%), ramipril (15%), aspirin (28.62%), and hydrochlorothiazide (5.86%)	Acetone and dimethyl sulfoxide (DMSO)	RegenHU 3D printer	Polypill [58]
Sucrose, Pectin, and Maltodextrin	Isoleucine (14.4%)	Water	Adapted 3D printer (The Magic Candy Factory, UK)	Chewable printlets [60]
Mesoporous Silica Nanoparticles (Msn) and Bioactive Glass Coatings in a Porous β-TCP Bioceramic	Isoniazid (INH)/ Rifampin (RFP)	Chloroform and dimethyl sulfoxide (DMSO)	3D-Bioplotter system, EnvisionTEC, Germany	Porous scaffold [63]
HPC and PVA	Warfarin (1.3%)	Ethanol and purified water	BioBots 1 (BioBot, USA) EXT 3D	Orodispersible film (ODF) [61]
Sodium Alginate and Hydroxyapatite	Insulin	Water	Allevi 2 bioprinter	Microneedle patches [54]

and repeating the fusion process. Depending on the equipment used, different mechanisms exist for this powder spreading. The most common method is the use of a metallic blade, a roller, or a rake for generating a powder layer with a precise layer height. API is typically incorporated into the powder blend but can also be added to the liquid binder in BJ printing [64]. After printing, loose powder is removed and recycled, revealing the printed structure. Further drying or curing is often necessary to further strengthen the print. Compared to other 3DP techniques, print surface finish and resolution is poor due to the rough nature of the powder feedstock and prints are fairly porous due to the loose packing of powder. Whilst less suitable for high strength, load bearing applications, the fairly weak binding and porous nature of PBF solid dosage forms can be advantageous for immediate release applications that require rapid dissolution. Porous, hygroscopic structures can be easily penetrated and broken down by liquids, making PBF prints well suited for oral delivery

applications. This feature is seen in the only currently Food and Drug Administration (FDA) approved 3D-printed pharmaceutical product, Spritam, which is manufactured using a proprietary BJ technology and undergoes rapid disintegration (~10 seconds) when taken with a sip of liquid [65].

Powder is an attractive feedstock for 3DP because pharmaceutical materials are already widely available in this form factor, so can be directly used in PBF techniques, simplifying the production process. The direct use means powder properties play a key role concerning both processing performance and part properties that require careful consideration for successful printing. Figure 1.3 shows some of the relationships between powder properties and bulk powder behaviour on in-process printing performance and final print properties. Of these properties, powder flowability, packing density, and energy absorbance are the key attributes that determine formulation printability.

1.2.3.1 Powder Flowability Considerations

In PBF, good flow properties are required to ensure that a homogenous, thin layer of fresh powder is distributed during spreading at the start of each layer. Small particles (<20 μm), which are desirable for higher resolution printing, are particularly challenging to process due to their relatively large specific surface area that results in a high extent of adhesiveness to surfaces and other particles due to van der Waal interactions [67]. General methods of improving powder flowability are decreasing the width of the powder size distribution (PSD) [68, 69], increasing particle sphericity and smoothness [70], increasing particle size [71], decreasing moisture content [72], and addition of flow enhancers [73]. To enhance the particle morphology of the PBF feedstock, it can be pre-processed by grinding, milling, or

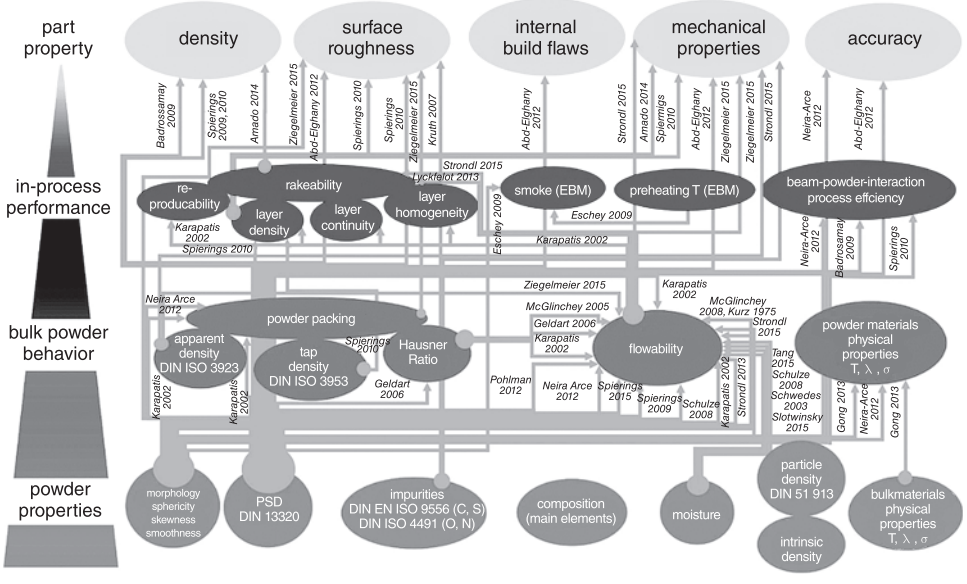

Figure 1.3 *Visualisation of the relationships between powder properties, bulk powder behaviour, powder performance in process, and finally, the manufactured part quality as elaborated by different research groups. (Source: Reproduced under the Creative Commons Attribution 4.0 International License [66].)*

spray drying [74, 75]. To obtain an even particle size distribution, it is recommended to sieve the feed powder prior to its use [76].

1.2.3.2 Powder Packing Density Considerations

The packing density of the powder feedstock has a strong influence on the final print density, surface roughness, and mechanical properties. A wide multimodal PSD is necessary to achieve a high powder bulk density, as the fine particles can fill the gaps between the larger ones. This is contradictory to the necessities for good powder flow and illustrates how contradictory the requirements for only one parameter can be with respect to different aspects of the PBF process. For high-strength applications such as bone tissue scaffolds, a high packing density is required to produce dense parts, whereas for pharmaceutical applications, low density prints are desirable to enhance tablet disintegration and drug release rates [77].

1.2.3.3 Powder Energy Absorbance Considerations

Powder energy absorbance describes the feedstocks' ability to absorb energy and bind to adjacent particles during printing. For the case of BJ printing, the energy absorbance refers to the interaction of the powder with the binder fluid. Binder deposition and spread is dependent on the viscosity, surface tension, and density of the binder solution and the wettability and specific surface area of the powder material [78]. In SLS printing, the energy absorbance is the feedstocks' capacity to absorb the wavelength of the laser used during printing. BJ has been shown to be effective for printing high-dose hydrophilic formulations for rapid disintegration [64, 79]. However, achieving good print quality can be a challenge when it comes to printing large doses of hydrophobic molecules which require water-based binders. Poor selection of a binder and powder bed properties may result in sliding of powder layers during printing and a decrease in the final product quality [80]. Formulating binders using a mixture of water and organic solvents can be used to overcome this but creates the problem of efficient removal of toxic solvent from the final formulation. In SLS printing, powder binding is dependent on the power and wavelength of the laser source, the laser energy absorptivity of the powder material, and the scanning speed [81, 82]. Increased laser power or decreased scanning speed increases powder particles exposure to the laser, increasing the level of sintering between particles. By tuning these parameters, part strength and porosity can be controlled which in turn mediate drug performance. For example, paracetamol loaded HPMC tablets have been printed at 100, 200, and 300 mm s^{-1} to achieve controlled drug release over 4, 3, and 2 hours, respectively [83]. Furthermore, scanning power and speed can be adjusted during a single print to create variable density dosage forms. This method was first used with biodegradable polymers by Leong et al. in 2006 [82]. The group printed PCL and poly(L-lactic acid) (PLLA) tablets with a denser outer region to act as a diffusion barrier and a more porous inner region to encapsulate the drug and achieve zero-order release. Additionally, it is important to consider the energy absorbance range of a powder feedstock. Typically, CO_2 laser diodes emit energy in the visible light region. Since most pharmaceutical polymers are white in colour, minimal energy absorption will occur naturally. As such, pharmaceutical grade colourants can be incorporated into the powder feedstock to facilitate the absorption of energy. Due to the localised heating used in SLS printing, there are concerns about the degradation of API during printing. Several studies have reported minimal drug degradation using fairly stable API such as paracetamol [84], ibuprofen [85], and progesterone [86], but there is no evidence to suggest

thermolabile API can be employed with this technique. Table 1.3 provides example formulas used in powder bed fusion 3D printing of pharmaceuticals and devices.

1.2.4 Stereolithography 3D Printing

Stereolithography (SLA) was one of the first 3D-printing techniques introduced as a commercial system, when Charles W. Hull filed a patent for the photopolymerisation technology in 1986 [91]. SLA 3D parts are constructed from a vat of liquid photopolymer resin that is cured in a layer-by-layer fashion by an ultraviolet light source. Two different methods of irradiation may be applied to stereolithography, laser-based SLA, and digital light projection DLP. The laser-based method selectively cures the liquid photopolymer in a point-to-point fashion, whilst in DLP, the UV light source is projected to expose and polymerise an entire layer at once. For subsequent layers, the build plate is raised by one layer thickness and the process is repeated until the full 3D designed part is exposed. As a light-based technique, SLA printing offers the highest resolution amongst 3D-printing technologies, with XY resolutions and layer heights generally between 25 μm and 100 μm [92]. As such, SLA is commonly used for applications where a high level of detail is required. Following print completion, parts typically need to undergo two post processing steps: washing, most commonly in isoporopyl alcohol (IPA) to rinse off liquid resin, followed by UV curing to improve the mechanical properties of the printed structure, since the photopolymerisation of the resins during printing is usually incomplete. The main limitation of the SLA technique is the restrictive availability of biocompatible, photocurable materials. Only a few materials are currently available, limiting the flexibility of the technology for printing materials with different release properties.

The SLA technology is based on the phenomenon of photopolymerisation (shown in Figure 1.4). Photopolymerisation is the use of light in order initiate a polymerisation reaction, converting a liquid monomer resin into a solid polymer. The polymerisation reaction is initiated by the addition of light-sensitive compounds called photoinitiators, which become active under the appropriate wavelengths, creating free radicals due to the conversion of the absorbed light energy [93]. These free radicals are then consumed in the reaction converting the liquid monomer into a solid state, which may be referred to as a crosslinked hydrogel [94].

SLA is used to date the least studied 3DP technique in drug delivery device manufacture, which can be mainly attributed to the limited availability of biocompatible photocurable materials. As an additional drawback, the SLA printers operate primarily with single materials. Thus, the fabrication of formulations with multiple materials, such as polypills, is limited. Despite these limitations, the technique has intriguing advantages over some of the other 3DP processes as a high resolution, non-thermal process that appears promising for printing personalised implants [96], transdermal delivery systems [97, 98], and oral tablets [99]. In transdermal drug delivery, the SLA method has been shown to be suitable for preparing microneedles with various shapes, sizes, and antimicrobial coatings. The high printing precision of SLA enables great accuracy and reproducibility, making it well suited to more demanding applications in terms of both accurate dosing and geometry [100–102]. Although SLA material availability for DDD applications is limited, there is some capacity for altering the mechanical properties of the material. Goyanes et al. prepared drug-eluding topical patches with salicylic acid according to a scanned image of an individual's nose [101]. The flexibility of the nose-shaped patches was adjusted by controlling the degree of crosslinking between PEGDA chains with the addition of poly(ethylene glycol) (PEG) as a filling agent. The first application of SLA in the formulation of 3D-printed tablets was described by Wang

Table 1.3 *Example materials used in powder bed fusion 3D printing of pharmaceutical solid dosage forms and devices.*

Powder bed fusion type	Polymer	Binder ink		Drug	Printer	Application
		Binder	Solvent			
BJ	Maltitol, maltodextrin, PVP	PVP	Aqueous buffer	Captopril (in binder)	TheriForm process	Immediate release tablet [64]
	Kollidon SR and HPMC	PVP, Tween 20, triethyl citrate	Water, Ethanol	Pseudoephedrine hydrochloride (in binder)	TheriForm process	Controlled release tablet [79]
	Lactose, PVP, mannitol	PVP	Water, Ethanol	Paracetamol (in powder bed)	Fochif Mechatronics Technology (China)	Fast disintegrating tablet [87]
	D-sucrose, pregelatinised starch, povidone K30, microcrystalline cellulose, and silicon dioxide	PVP	Ethanol	Warfarin sodium (in powder bed)	Fochif Mechatronics Technology (China)	Oral disintegrating tablet [88]
	Tricalcium phosphate powder		Phosphoric acid	Vancomycin, ofloxacin, and tetracycline (post print impregnation)	3D-powder printing system (Z-Corporation, USA)	Microporous bioceramic implants [89]
SLS	Kollicoat IR and Eudragit L100–55, Candurin® Gold Sheen	N/A	N/A	Paracetamol	Sintratec Kit, AG, Brugg, Switzerland	Controlled release tablets [84]
	Hydroxypropyl methylcellulose (HPMC E5) and Kollidon® VA 64, Candurin® Gold Sheen	N/A	N/A	Paracetamol	Sintratec Kit, AG, Brugg, Switzerland	Immediate release tablets [83]
	Polyethylene	N/A	N/A	Progesterone and fluorouracil		Intrauterine drug delivery [90]

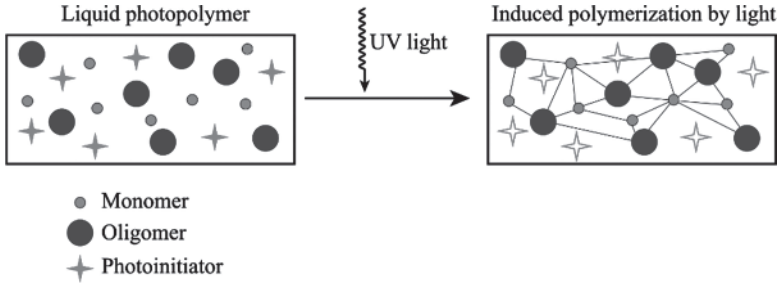

Figure 1.4 *Process of photopolymerisation. Crosslinking of monomers, oligomers, and photoinitiator liquid resin upon exposure to UV light to produce a solid material. (Source: Reproduced under the Creative Commons Attribution 4.0 International License. [95].)*

Table 1.4 *Example materials used in SLA for 3D printing of pharmaceuticals and devices.*

Polymer	Drug	Photoinitiator	Printer	Application
Polyethylene Glycol Diacrylate	Ibuprofen	DPPO	Formlabs 1 + SLA	Hydrogel tablets [104]
Poly(Ethylene Glycol) Diacrylate (PEGDA)	Acetylsalicylic acid	Darcure 2959	Home made	Tissue scaffold [105]
Polyethylene Glycol Diacrylate (PEGDA)	4-aminosalicylic acid (4-ASA) and paracetamol (acetaminophen)	DPPO	Form 1+ SLA 3D	Controlled release tablet [100]
Poly(2-Hydroxyethyl Methacrylate) (pHEMA), Poly(Ethylene Glycol) Dimethacrylate (PEGDMA)	Methylene blue hydrate	TPO		Subcutaneous implants [106]
Formlabs Elastic Resin	Lidocaine	(formulated in the commercial resin)	Form 2 SLA 3D	Bladder device for intravesical drug delivery [107]

et al., who produced dosage forms in a torus geometry using a photosensitive resin consisting of polyethylene glycol diacrylate 700 (PEGDA 700) and diphenyl (2,4,6-trimethylbenzoyl) phosphineoxide (TPO) as a photoinitiator [100]. The loading of paracetamol and 4-ASA in the printed tablets was 5.69% and 5.40%, respectively. To be able to manufacture DDD with higher drug loadings, the API must be adequately soluble in the polymer, which restricts the use of SLA for high-dose DDD. However, the manufacturing of printable objects with homogenously suspended particles (with loadings up to 53%) has been reported [103]. This indicates that the SLA printing of DDS from resins containing undissolved drug particles at higher drug content could be possible. Table 1.4 gives examples of combinations of polymer and photoinitiators used for pharmaceutical and medical device printing.

1.3 Classification of Common Materials Used in Pharmaceutical 3DP

In today's medicine, API carrier materials such as polymers and lipids form the basis of modern advanced delivery systems, having a multifaceted role on both the processability and functionality of a formulation. Suitable materials should be biocompatible, not negatively interact with the API, amenable to control API release profile, and printable. As such, the requirements are often different, depending on the printing technology used and intended application. Polymers are the most versatile category of biomaterials and have found use in the pharmaceutical industry as binders, lubricants, fillers, and solubility enhancers in solid dosage form production. Polymers are macromolecules composed of repeating units of monomers, which can either be naturally occurring, synthetically modified, or synthetically manufactured [108]. This section reviews the most common materials used in pharmaceutical 3DP as drug carriers and their key characteristics that influence processability and API function. It is important to bear in mind that the addition of API or additional excipients will have a significant effect on the thermal, rheological, and functional properties of a formulation but material choice is an important starting point that can be used to determine the necessity of additional excipients.

1.3.1 Alcohol Derived Polymers

- **Polyvinyl Alcohol (PVA) –** Polyvinyl alcohol (PVA), a water-soluble crystalline material that is easily biodegradable and considered a safe pharmaceutical excipient, is already used in multiple market drug delivery systems [109, 110]. Depending on the degree of hydrolysis of the acetate groups, the melting point of PVA may range from 180 °C (partially hydrolysed) to 228 °C (fully hydrolysed). It has a glass transition temperature of 85 °C [111] and begins to thermally degrade above 200 °C [112]. PVA is one of the most commonly used thermoplastics for 3DP and can be used with TE, PAM, and BJ [113–115].
- **Polyvinylpyrrolidone (PVP) –** Polyvinylpyrrolidone (PVP) is an amorphous non-ionic polymer made from repeating units of *N*-vinylpyrrolidone with good solubility in water and other polar solvents. PVP grades are labelled with K-values that relate to the molecular weight and degree of polymerisation and crosslinking of the material. PVP T_g is between 72 °C and 177 °C, dependent on the grade used with a degradation temperature of between 166 °C and 217 °C [116].
- **Poly(vinylpyrrolidone)/vinyl acetate (PVPVA) –** PVP can be crosslinked with vinyl acetate to form a PVPVA copolymer with is insoluble in water. It has a T_g of 105 °C and a T_{deg} of 270 °C [116]. PVPVA presents a molecular weight above 70 kDa and is widely used in pharmaceutical formulations as a direct compression, tablet disintegrant, film-forming, and taste-masking excipient, also known for its suitability for HME.

1.3.2 Eudragits

Eudragits are methacrylic polymers that were first introduced in the 1950s for enteric coatings. They are amorphous polymers that can achieve a wide range of targeted release profiles, depending on the functional groups incorporated into them. Eudragit E is suitable for immediate release in the stomach, dissolving in acidic conditions below pH 5. Alternatively, Eudragit L and S have been developed for targeted release to the gastrointestinal tract and

colon at pH values of above 6 and 7, respectively, withstanding the acidic environment of the stomach [117]. Eudragit RS and RL are polymers with similar sustained release properties but suitable for pH independent release applications. Eudragit materials are commonly utilised using thermal deposition 3D-printing techniques due to their good thermal characteristics, although plasticisation is often necessary to reduce the melt viscosity of the formulations. Glass transition temperature and thermal degradation onset temperature for Eudragit E, RL, RS, L, and S are 52 °C and 250 °C [118], 63 °C and 166 °C, 64 °C and 170 °C [119], 157 °C and 206 °C, and 163 °C and 188 °C [120], respectively. Due to their versatile release characteristics, Eudragit has been used to optimise drug delivery for a variety of applications, including ophthalmic [121], buccal or sublingual [122], enteric [123], oral [40], colon [124], vaginal [125], and transdermal [126] delivery. Although Eudragit is most frequently used for thermal extrusion 3DP, it has also been used with powder bed fusion technologies [127, 128]

1.3.3 Other Polymers

- **Polycaprolactone (PCL) –** PCL is a semi-crystalline, biodegradable polyester which has received a great deal of interest for use as an implantable biomaterial. PCL undergoes slow degradation by hydrolysis of its ester linkages under physiological conditions (such as the human body), so is widely used in long-term implants and controlled drug release applications [129]. With a low melting point and glass transition temperature of 60 °C and −60 °C respectively and a high T_{deg} of 310 °C [23], PCL has great properties for HME and FDM printing and is a commonly used filament feedstock in addition to excellent solubility in organic solvents. PCL is considered a good elastic biomaterial due to its low tensile strength (~0.023 GPa) and high elongation at breakage (4700%) [130].
- **Ethylene vinyl acetate (EVA) –** EVA is the copolymer of semi-crystalline ethylene and amorphous vinyl acetate that produces materials with a 'rubber-like' feel. The weight percentage of vinyl acetate usually varies from 10% to 40%, with decreased percentage grades corresponding to increased thermal and mechanical properties. EVA has a T_g of −28 °C and a high T_{deg} of 300 °C [131].
- **Polyethylene glycol (PEG) –** PEG, also known as PEO, depending on its molecular weight, is a water soluble, highly crystalline, biocompatible, amphiphilic polymer that is widely used as an excipient in many pharmaceutical products. Polymers with Mw <100,000 are usually called PEGs, while higher molecular weight polymers are classified as PEOs. PEG has a T_g of −56 °C, a T_m of 57 °C to 63 °C, and a T_{deg} of 330 °C [132].
- **Polyglycolic acid (PGA), Polylactic acid (PLA) and their co-polymers –** PGA and PLA are both semi-crystalline, highly biocompatible polymers which have been extensively researched and utilised for long-term (months to years) medical implants and drug delivery scaffolds [133]. Both thermoplastic materials degrade by hydrolysis under physiological conditions into lactic acid and glycolic acid, which are both natural by-products of metabolic pathways in the body. They are commonly used for long-term implants such as pins, rods, plates, sutures [134], and tissue engineering scaffolds. Biodegradable implants are hugely beneficial for support structures because they gradually transfer the load to the body as it heals and does not require further surgery for removal. PLA has two pharmaceutically relevant forms, PLLA and poly(DL-lactide) (PDLLA). PLLA has a T_g of 60 °C to 65 °C, T_m of 175 °C, and strength of 4.8 GPa; whereas, PDLLA has a slightly lower T_g of 55 °C to 60 °C and a mechanical strength of 1.9 GPa [135]. Both forms thermally degrade above

300 °C [136]. PGA has a glass transition temperature between 35 °C and 40 °C and its melting point is reported to be in the range of 225 °C to 230 °C and begins to degrade at approximately 250 °C [137]. Poly(lactic acid-co-glycolic acid) (PLGA) is a copolymer of PLA and PGA that has favourable degradation mechanics, which can be tuned depending on the ratio of lactide to glycolide used for the polymerisation. The higher the content of glycolide units, the lower the time required for degradation as compared to predominantly lactide materials. An exception to this rule is the copolymer with a 50:50 monomers' ratio, which exhibits faster degradation (about two months). PLGAs typically show similar thermal properties to PLA and PGA, with a glass transition in the range of 40 °C to 60 °C.

1.3.4 Graft Polymers

- **Soluplus® –** is a swellable, non-ionic water-soluble graft polymer comprised of PCL, PVA, and PEG, which exhibits amphiphilic properties. It has a large number of hydroxyl groups that make it a great solubiliser for BCS class II drugs in aqueous media and for creating amorphous dispersions [138]. It has a low T_g of 70 °C and a high T_{deg} of 278 °C [139], making it a good candidate for HME, although plasticisation is often required to reduce the brittleness of extruded filament [140].
- **Carbopol® –** is a high molecular weight polymer composed of polyacrylic acid crosslinked with allyl sucrose or allyl pentaerythritol. The crosslinking degree determines the viscosity of the polymer. It can be incorporated into drug loaded paste formulations for PAM printing, generally used to provide sustained release [47]. Carbopol 971P, a lightly crosslinked formulation, has a viscosity range of 4,000 cP to 11,000 cP (or mPa.s) and Carbopol 974P, a highly crosslinked formulation, has a viscosity range of 29,400 cP to 39,400 cP [141].
- **Kollicoat® IR –** is a robust yet flexible PVA/polyethylene glycol graft copolymer that is rapidly water soluble and commonly used for manufacturing immediate release coatings and solid dosage forms. It has a T_g of 48 °C, a T_m of 208 °C, and a T_{deg} of 200 °C [116].

1.3.5 Photocrosslinkable

Over the past few years, a number of photocrosslinkable polymers have been developed suitable for drug delivery, such as poly(ethylene glycol) diacrylate (PEGDA), poly(2-hydroxyethyl methacrylate) (pHEMA), poly(ethylene glycol) dimethacrylate (PEGDMA), and poly(propylene fumarate)/diethyl fumarate (PPF/DEF). Typically, a photopolymer consists of a mixture of monomers and photoinitiators which, when exposed to UV light, crosslink to form a solid material. PEG-based polymers are water soluble whereas pHEMA is an insoluble but swellable material. PPF/DEF has emerged as a useful photocurable, biodegradable material for manufacturing high strength structures for applications in bone tissue engineering [142].

1.3.6 Natural Materials

Due to their abundance in nature and favourable properties (low-cost, biocompatibility, and biodegradability), polysaccharides have received increased attention in a wide range of applications, including pharmaceuticals. Their intrinsic properties can be easily tuned through chemical modification (increase solubility, change hydrophilic/hydrophobic balance, etc.) and further improved by combining them with other carefully chosen natural or synthetic

polymers. Polysaccharides are susceptible to crosslinking, which can be implemented to maintain the structural integrity of the printed objects, increase their mechanical properties, or delay their degradation. Moreover, polysaccharides bearing ionic groups can exhibit a responsive behaviour, e.g., pH-responsive for chitosan, that allows for an additional level of control [143].

- **Cellulose derived polymers –** Cellulose is a highly hydrophilic polymer, although it is water insoluble due to its high degree of crystallinity and structure. For this reasons, cellulose is typically modified to form derivatives, such as Ethyl cellulose (EC), Hydroxypropyl cellulose (HPC), Hydroxypropyl methylcellulose (HPMC), and Hydroxypropyl methylcellulose Acetate Succinate (HPMCAS), with better release and processability properties. Cellulose-derived polymers are widely used in TE and SSE printing as a controlled release matrix (high molecular weight) or as a binder (low molecular weight). HPC and HPMC are amorphous, swellable, hydrophilic water-soluble polymers that exhibit pH independent release. EC is semi-crystalline and not water soluble. HPMCAS is amorphous and anionic, insoluble in gastric fluid but swells and dissolves rapidly in neutral to mildly alkaline pH. Therefore, HPMC is often used as a enteric coating material [144] and for sustained release applications [145]. Glass transition temperatures and thermal degradation onset temperatures for EC, HPC, HPMC, and HPMCAS are 130 °C and 200 °C [146], 111 °C and 227 °C [147], 96 °C to 145 °C (dependant on molecular weight) and 220 °C [148], and 115 °C and 260 °C, respectively. All but EC are amorphous, which has a melting peak at 170 °C. Cellulose-based polymers are widely used in pharmaceutical formulations because of their capability to stabilise suspensions and emulsions, form films in coating formulations, act as thickening/bonding agent, and resist hydrolysis in gastrointestinal tract [149].
- **Chitosan –** Chitosan is a natural product obtained from the shells of crustaceans such as shrimps and crabs. It is a very versatile polysaccharide with good antimicrobial and mucoadhesive properties due to the positive charge of its amino group. Pure chitosan hydrogels can be printed using SSE technologies but to improve mechanical strength an additional crosslinking step is often required. Mechanical properties can also be improved by blending with other natural polymers such as sodium alginate and pectin. The negatively charged carboxyl group of sodium alginate and pectin forms polyelectrolyte complexes with chitosan, which significantly increase the viscosity of the formulation, improving shape fidelity after printing [150].
- **Pectin –** Pectin is another anionic polysaccharide that is commonly used as a thickening agent.
- **Alginate –** Alginate (Alg) is an anionic linear polysaccharide constituted of units of β-d-mannuronic acid and its epimer α-l-guluronic acid. Similar to chitosan, Alg has good gelling properties that are appropriate for SSE, but a post processing crosslinking step is often required. Alg chains can be easily crosslinked in the presence of divalent ions, notably Ca^{2+}.
- **Collagen and Gelatin –** Collagen is an insoluble, swellable structural protein composed mainly of glycine, proline, and hydroxyproline residues. Gelatin is an swellable anionic polymer, produced by the partial degradation of collagen that is soluble at and above physiological temperatures (37 °C) [151]. Both materials form hydrogels and have shown promise in SSE tissue engineering applications [152, 153].

1.3.7 Lipid Materials

Lipid-based excipients are obtained from vegetable oils, waxes, or fatty acids. They have recently been explored for pharmaceutical 3DP due to their ability to enhance the bioavailability of poorly soluble drugs. Lipids can do this by maintaining the drugs in the solubilised

state, modifying gastric emptying, and by changing the drug distribution post absorption [154–157]. In addition, the degradation products of lipids can interact with endogenous components (i.e., bile salt, phospholipid, and cholesterol) and form a variety of colloidal structures that can act as a transport medium for the absorption of lipophilic drugs [158]. Lipids typically have a low melting temperature, so can be processed using thermal extrusion 3DP, quickly solidifying after printing. Gelucire® with Koliphor®, as surfactants, have been used to print drug loaded self-microemulsifying drug delivery systems (SMEDDS) for oral drug delivery. Theobroma oil (cocoa butter), the major ingredient in chocolate, has also been used for printing paediatric friendly formulations at low temperatures (45 °C) using corn syrup as a thickening agent [159]. Besides oral dosage forms, SMEDDS have also be employed to prepare suppositories based on coconut oil [160]. Recently, a similar thermal inkjet printing technique has been using to print high resolution beeswax tablets with complex microstructure geometry [161].

It should be highlighted that in most formulations of 3D-printed pharmaceuticals and devices, functional excipients are used to aid the processability and/or drug delivery performance (i.e., drug release rate, taste masking, solubility enhancement). Table 1.5 gives examples of functional excipients used in pharmaceutical 3D printing.

Table 1.5 *Additional functional excipients used in pharmaceutical 3DP.*

Excipient	Function	Examples
Plasticiser	Plasticisers are smaller molecules that act as a lubricant between segments of polymer chains increasing the material's flexibility and softness	Triethyl citrate [23, 162], Glycerol [163], Sorbitol [164], Kolliphor [165], TPGS [165], PEG [118], PEO [118], Mannitol, and Tween 80, API also often have a plasticising effect on the formulation, which can be significant, especially at high drug loadings [166]
Ph and Release Modifiers	Speed up, slow down, or control the release of the API	• Disintegrant – Kollidon CL-F [139], Tri-calcium phosphate [167], Sodium starch glycolate [168], Croscarmellose [168] • Channelling agent – Mannitol [23] • pH dependant – tribasic phosphate sodium [162]
Processing Aids	Reduce the tackiness of the formulation	PEG 6000 [23], dibutyl sebacate [169], Talc [162], magnesium stearate [170], magnesium carbonate, Sodium [20], Lauril Sulfate [168], Calcium stearate [171]
Solubility Enhancer	Enhance the amount of API that can be dissolved in formulation	Soluplus [172], PVP [173], Tween 80 [118]
Taste Masking	Delay the release of bitter API until after swallowing	Eudragit EPO [174]
Crystallisation Inhibitors	Slow the recrystallisation of API after amorphorisation	Polycarbophil [31], (PVP) K25 [31], poloxamer 188 [31], PEG3350[31]
Colorants	Change the colour of extruded material for aesthetic reasons or to increase UV/laser energy absorbance	Candurin Orange Amber [175], Candurin Gold Sheen [175], Food Colouring [175]

1.4 Conclusions and Future Perspectives

A wide range of materials, printing technologies, and applications have been covered in this chapter, giving insight into the material considerations necessary when designing a new DDD. Traditionally, material formulation optimisation has been done using a trial-and-error approach to establish which formulations are printable. However, as the research space has matured, so has understanding on the material properties that influence printability and drug release function. Rheology has shown to be a powerful predictive tool for predicting formulation printability and even drug release profiles for nozzle-based systems (TE, SSE, BJ), whilst, for powder-based systems (BJ and SLS), good powder flowability is critical for continuous printing. Material requirements for TE, SSE, PBF, and SLA 3DP are very different due to vastly differing printing conditions. As such, there is no single 'one' technique which is best suited for all drug delivery applications. Instead, specific application requirements (release properties, mechanical stability, design complexity, etc.) should be considered along with the API stability to target the most suitable 3DP technology and API carrier materials. As pharmaceutical 3DP becomes a more mature technology, we are seeing increased research effort, both in creating new materials specifically for improved printability and API solubilising potential, as well as more versatile printing technologies with less restrictive printability windows (i.e., granule/powder direct thermal deposition systems).

3D printing of pharmaceuticals has been shown to be advantageous for manufacturing personalised medicine, offering design flexibility, high complexity, on-demand, and cost-effective production. Whilst there are still challenges associated with the limited availability of excipients, the vast quantity and variability of drug delivery systems developed within the pharmaceutical 3DP literature suggests this is not the major factor delaying the adoption of pharmaceutical 3DP in industry. Wider technical challenges around the development of printing software, scalability, and the regulatory landscape still need to be overcome before the large-scale production of 3DP pharmaceutical is widespread.

References

[1] van der Vossen, A.A.-O., Al-Hassany, L., Buljac, S. et al. (2019). Manipulation of oral medication for children by parents and nurses occurs frequently and is often not supported by instructions. *Acta Paediatrica* **108** (1651–2227): 1475–1481.

[2] Martir, J., Flanagan, T., Mann, J., and Fotaki, N. (2017). Impact of co-administration of food and drink vehicles on the solubility of poorly soluble paediatric drugs.

[3] Palo, M., Holländer, J., Suominen, J. et al. (2017). 3D printed drug delivery devices: perspectives and technical challenges. *Expert Review of Medical Devices* **14** (9): 685–696.

[4] Seoane-Viaño, I., Januskaite, P., Alvarez-Lorenzo, C. et al. (2021). Semi-solid extrusion 3D printing in drug delivery and biomedicine: personalised solutions for healthcare challenges. *Journal of Controlled Release* **332**: 367–389. https://doi.org/10.1016/j.jconrel.2021.02.027.

[5] Prasad, L.K. and Smyth, H. (2016). 3D printing technologies for drug delivery: a review. *Drug Development and Industrial Pharmacy* **42** (7): 1019–1031. https://doi.org/10.3109/03639045.2015.1120743.

[6] West, T.G. and Bradbury, T.J. (2019). 3D printing: a case of ZipDose® technology–world's first 3D printing platform to obtain FDA approval for a pharmaceutical product. *3D and 4D Printing in Biomedical Applications: Process Engineering and Additive Manufacturing* 53–79.

[7] Ghanizadeh Tabriz, A., Nandi, U., Hurt, A.P. et al. (2021). 3D printed bilayer tablet with dual controlled drug release for tuberculosis treatment. *International Journal of Pharmaceutics* **593**: 120147. https://doi.org/10.1016/j.ijpharm.2020.120147.

[8] Goole, J. and Amighi, K. (2016). 3D printing in pharmaceutics: a new tool for designing customized drug delivery systems. *International Journal of Pharmaceutics* **499** (1): 376–394. https://doi.org/10.1016/j.ijpharm.2015.12.071.

[9] Zhang, B., Gleadall, A., Belton, P. et al. (2021). New insights into the effects of porosity, pore length, pore shape and pore alignment on drug release from extrusion-based additive manufactured pharmaceuticals. *Additive Manufacturing* **46**: 102196. https://doi.org/10.1016/j.addma.2021.102196.
[10] Long, J., Gholizadeh, H., Lu, J. et al. (2017). Application of fused deposition modelling (FDM) method of 3D printing in drug delivery. *Current Pharmaceutical Design* **23** (3): 433–439.
[11] Tan, D.K., Maniruzzaman, M., and Nokhodchi, A. (2018). Advanced pharmaceutical applications of hot-melt extrusion coupled with fused deposition modelling (FDM) 3D printing for personalised drug delivery. *Pharmaceutics* **10** (4): 203.
[12] Okwuosa, T.C., Stefaniak, D., Arafat, B. et al. (2016). A lower temperature FDM 3D printing for the manufacture of patient-specific immediate release tablets. *Pharmaceutical Research* **33** (11): 2704–2712.
[13] Alshahrani, S.M., Morott, J.T., Alshetaili, A.S. et al. (2015). Influence of degassing on hot-melt extrusion process. *European Journal of Pharmaceutical Sciences* **80**: 43–52.
[14] Li, S., Tian, Y., Jones, D.S., and Andrews, G.P. (2016). Optimising drug solubilisation in amorphous polymer dispersions: rational selection of hot-melt extrusion processing parameters. *AAPS Pharmscitech* **17** (1): 200–213.
[15] Aho, J., Boetker, J.P., Baldursdottir, S., and Rantanen, J. (2015). Rheology as a tool for evaluation of melt processability of innovative dosage forms. *International Journal of Pharmaceutics* **494** (2): 623–642.
[16] Thiry, J., Krier, F., and Evrard, B. (2015). A review of pharmaceutical extrusion: critical process parameters and scaling-up. *International Journal of Pharmaceutics* **479** (1): 227–240.
[17] Yang, Y., Wang, H., Li, H. et al. (2018). 3D printed tablets with internal scaffold structure using ethyl cellulose to achieve sustained ibuprofen release. *European Journal of Pharmaceutical Sciences* **115**: 11–18.
[18] Moseson, D.E. and Taylor, L.S. (2018). The application of temperature–composition phase diagrams for hot melt extrusion processing of amorphous solid dispersions to prevent residual crystallinity. *International Journal of Pharmaceutics* **553** (1): 454–466. https://doi.org/10.1016/j.ijpharm.2018.10.055.
[19] Verstraete, G., Samaro, A., Grymonpré, W. et al. (2018). 3D printing of high drug loaded dosage forms using thermoplastic polyurethanes. *International Journal of Pharmaceutics* **536** (1): 318–325.
[20] Kollamaram, G., Croker, D.M., Walker, G.M. et al. (2018). Low temperature fused deposition modeling (FDM) 3D printing of thermolabile drugs. *International Journal of Pharmaceutics* **545** (1): 144–152. https://doi.org/10.1016/j.ijpharm.2018.04.055.
[21] Goyanes, A., Buanz, A.B.M., Basit, A.W., and Gaisford, S. (2014). Fused-filament 3D printing (3DP) for fabrication of tablets. *International Journal of Pharmaceutics* **476** (1–2): 88–92.
[22] Tagami, T., Fukushige, K., Ogawa, E. et al. (2017). 3D printing factors important for the fabrication of polyvinyl-alcohol filament-based tablets. *Biological and Pharmaceutical Bulletin* **40** (3): 357–364.
[23] Beck, R.C.R., Chaves, P.S., Goyanes, A. et al. (2017). 3D printed tablets loaded with polymeric nanocapsules: an innovative approach to produce customized drug delivery systems. *International Journal of Pharmaceutics* **528** (1): 268–279. https://doi.org/10.1016/j.ijpharm.2017.05.074.
[24] Ibrahim, M., Barnes, M., McMillin, R. et al. (2019). 3D printing of metformin HCl PVA tablets by fused deposition modeling: drug loading, tablet design, and dissolution studies. *AAPS Pharmscitech* **20** (5): 1–11.
[25] Karalia, D., Siamidi, A., Karalis, V., and Vlachou, M. (2021). 3D-printed oral dosage forms: mechanical properties, computational approaches and applications. *Pharmaceutics* **13** (9): 1401.
[26] Goyanes, A., Buanz, A.B.M., Hatton, G.B. et al. (2015). 3D printing of modified-release aminosalicylate (4-ASA and 5-ASA) tablets. *European Journal of Pharmaceutics and Biopharmaceutics* **89**: 157–162. https://doi.org/10.1016/j.ejpb.2014.12.003.
[27] Kalepu, S. and Nekkanti, V. (2015). Insoluble drug delivery strategies: review of recent advances and business prospects. *Acta Pharmaceutica Sinica B* **5** (5): 442–453. https://doi.org/10.1016/j.apsb.2015.07.003.
[28] Loftsson, T. and Brewster, M.E. (2010). Pharmaceutical applications of cyclodextrins: basic science and product development. *Journal of Pharmacy and Pharmacology* **62** (11): 1607–1621. 10.1111/j.2042-7158.2010.01030.x.

[29] Vaka, S.R.K., Bommana, M.M., Desai, D. et al. (2014). Excipients for amorphous solid dispersions. In: *Amorphous Solid Dispersions*, 123–161. Springer.
[30] Crowley, M.M., Fredersdorf, A., Schroeder, B. et al. (2004). The influence of guaifenesin and ketoprofen on the properties of hot-melt extruded polyethylene oxide films. *European Journal of Pharmaceutical Sciences* **22** (5): 409–418.
[31] Bruce, C., Fegely, K.A., Rajabi-Siahboomi, A.R., and McGinity, J.W. (2007). Crystal growth formation in melt extrudates. *International Journal of Pharmaceutics* **341** (1–2): 162–172.
[32] Alhnan, M.A., Okwuosa, T.C., Sadia, M. et al. (2016). Emergence of 3D Printed Dosage Forms: Opportunities and Challenges. *Pharmaceutical Research* **33**: 1817–1832.
[33] Yu, D.G., Zhu, L.-M., Branford-White, C.J., and Yang, X.L. (2008). Three-dimensional printing in pharmaceutics: promises and problems. *Journal of Pharmaceutical Sciences* **97** (9): 3666–3690. https://doi.org/10.1002/jps.21284.
[34] Elbadawi, M., Gustaffson, T., Gaisford, S., and Basit, A.W. (2020). 3D printing tablets: predicting printability and drug dissolution from rheological data. *International Journal of Pharmaceutics* **590**: 119868. https://doi.org/10.1016/j.ijpharm.2020.119868.
[35] Solanki, N.G., Tahsin, M., Shah, A.V., and Serajuddin, A.T.M. (2018). Formulation of 3D printed tablet for rapid drug release by fused deposition modeling: screening polymers for drug release, drug-polymer miscibility and printability. *Journal of Pharmaceutical Sciences* **107** (1): 390–401. https://doi.org/10.1016/j.xphs.2017.10.021.
[36] Nasereddin, J.M., Wellner, N., Alhijjaj, M. et al. (2018). Development of a simple mechanical screening method for predicting the feedability of a pharmaceutical FDM 3D printing filament. *Pharmaceutical Research* **35** (8): 1–13.
[37] Elbadawi, M., Muñiz Castro, B., Gavins, F.K.H. et al. (2020). M3DISEEN: a novel machine learning approach for predicting the 3D printability of medicines. *International Journal of Pharmaceutics* **590**: 119837. https://doi.org/10.1016/j.ijpharm.2020.119837.
[38] Xu, P., Li, J., Meda, A. et al. (2020). Development of a quantitative method to evaluate the printability of filaments for fused deposition modeling 3D printing. *International Journal of Pharmaceutics* **588**: 119760. https://doi.org/10.1016/j.ijpharm.2020.119760.
[39] Goyanes, A., Allahham, N., Trenfield, S.J. et al. (2019). Direct powder extrusion 3D printing: fabrication of drug products using a novel single-step process. *International Journal of Pharmaceutics* **567**: 118471. https://doi.org/10.1016/j.ijpharm.2019.118471.
[40] McDonagh, T., Belton, P., and Qi, S. (2022). Direct granule feeding of thermal droplet deposition 3D printing of porous pharmaceutical solid dosage forms free of plasticisers. *Pharmaceutical Research* **39** (3): 599–610.
[41] Goyanes, A., Chang, H., Sedough, D. et al. (2015). Fabrication of controlled-release budesonide tablets via desktop (FDM) 3D printing. *International Journal of Pharmaceutics* **496** (2): 414–420. https://doi.org/10.1016/j.ijpharm.2015.10.039.
[42] Shi, K., Salvage, J.P., Maniruzzaman, M., and Nokhodchi, A. (2021). Role of release modifiers to modulate drug release from fused deposition modelling (FDM) 3D printed tablets. *International Journal of Pharmaceutics* **597**: 120315. https://doi.org/10.1016/j.ijpharm.2021.120315.
[43] Welsh, N.R., Malcolm, R.K., Devlin, B., and Boyd, P. (2019). Dapivirine-releasing vaginal rings produced by plastic freeforming additive manufacturing. *International Journal of Pharmaceutics* **572**: 118725. https://doi.org/10.1016/j.ijpharm.2019.118725.
[44] Genina, N., Holländer, J., Jukarainen, H. et al. (2016). Ethylene vinyl acetate (EVA) as a new drug carrier for 3D printed medical drug delivery devices. *European Journal of Pharmaceutical Sciences* **90**: 53–63. https://doi.org/10.1016/j.ejps.2015.11.005.
[45] Maroni, A., Melocchi, A., Parietti, F. et al. (2017). 3D printed multi-compartment capsular devices for two-pulse oral drug delivery. *Journal of Controlled Release* **268**: 10–18. https://doi.org/10.1016/j.jconrel.2017.10.008.
[46] Pereira, B.C., Isreb, A., Forbes, R.T. et al. (2019). Temporary plasticiser: a novel solution to fabricate 3D printed patient-centred cardiovascular 'Polypill' architectures. *European Journal of Pharmaceutics and Biopharmaceutics* **135**: 94–103. https://doi.org/10.1016/j.ejpb.2018.12.009.
[47] Khaled, S.A., Burley, J.C., Alexander, M.R., and Roberts, C.J. (2014). Desktop 3D printing of controlled release pharmaceutical bilayer tablets. *International Journal of Pharmaceutics* **461** (1–2): 105–111.
[48] Pandey, M., Choudhury, H., Fern, J.L.C. et al. (2020). 3D printing for oral drug delivery: a new tool to customize drug delivery. *Drug Delivery and Translational Research* **10** (4): 986–1001.

[49] Aguilar-de-leyva, Á., Linares, V.A.-O., Casas, M.A.-O., and Caraballo, I.A.-O. (2020). 3D printed drug delivery systems based on natural products. *Pharmaceutics* **12** (7): 620.
[50] Nourished personalised gummy vitamins (2022). https://get-nourished.com/. Accessed in Jan 2022.
[51] Cui, M., Pan, H., Fang, D. et al. (2020). Fabrication of high drug loading levetiracetam tablets using semi-solid extrusion 3D printing. *Journal of Drug Delivery Science and Technology* **57**: 101683. https://doi.org/10.1016/j.jddst.2020.101683.
[52] Wen, H., He, B., Wang, H. et al. (2019). Structure-based gastro-retentive and controlled-release drug delivery with novel 3D printing. *AAPS PharmSciTech* **20** (2): 68.
[53] Elkasabgy, N.A., Mahmoud, A.A., and Maged, A. (2020). 3D printing: an appealing route for customized drug delivery systems. *International Journal of Pharmaceutics* **588**: 119732. https://doi.org/10.1016/j.ijpharm.2020.119732.
[54] Wu, M., Zhang, Y., Huang, H. et al. (2020). Assisted 3D printing of microneedle patches for minimally invasive glucose control in diabetes. *Materials Science and Engineering: C* **117**: 111299. https://doi.org/10.1016/j.msec.2020.111299.
[55] Lewis, J.A. and Gratson, G.M. (2004). Direct writing in three dimensions. *Materials Today* **7** (7–8): 32–39.
[56] Jones, N. (2012). Science in three dimensions: the print revolution. *Nature* **487** (7405): 22–23.
[57] Zidan, A., Alayoubi, A., Coburn, J. et al. (2019). Extrudability analysis of drug loaded pastes for 3D printing of modified release tablets. *International Journal of Pharmaceutics* **554**: 292–301.
[58] Khaled, S.A., Burley, J.C., Alexander, M.R. et al. (2015). 3D printing of five-in-one dose combination polypill with defined immediate and sustained release profiles. *Journal of Controlled Release* **217**: 308–314.
[59] Real, J.P., Barberis, M.E., Camacho, N.M. et al. (2020). Design of novel oral ricobendazole formulation applying melting solidification printing process (MESO-PP): an innovative solvent-free alternative method for 3D printing using a simplified concept and low temperature. *International Journal of Pharmaceutics* **587**: 119653.
[60] Goyanes, A., Madla, C.M., Umerji, A. et al. (2019). Automated therapy preparation of isoleucine formulations using 3D printing for the treatment of MSUD: first single-centre, prospective, crossover study in patients. *International Journal of Pharmaceutics* **567**: 118497. https://doi.org/10.1016/j.ijpharm.2019.118497.
[61] Sjöholm, E. and Sandler, N. (2019). Additive manufacturing of personalized orodispersible warfarin films. *International Journal of Pharmaceutics* **564**: 117–123. https://doi.org/10.1016/j.ijpharm.2019.04.018.
[62] Khaled, S.A., Burley, J.C., Alexander, M.R. et al. (2015). 3D printing of tablets containing multiple drugs with defined release profiles. *International Journal of Pharmaceutics* **494** (2): 643–650.
[63] Zhu, M., Li, K., Zhu, Y. et al. (2015). 3D-printed hierarchical scaffold for localized isoniazid/rifampin drug delivery and osteoarticular tuberculosis therapy. *Acta Biomaterialia* **16**: 145–155. https://doi.org/10.1016/j.actbio.2015.01.034.
[64] Lee, K.-J., Kang, A., Delfino, J.J. et al. (2003). Evaluation of critical formulation factors in the development of a rapidly dispersing captopril oral dosage form. *Drug Development and Industrial Pharmacy* **29** (9): 967–979.
[65] Trenfield, S.J., Madla, C.M., Basit, A.W., and Gaisford, S. (2018). Binder jet printing in pharmaceutical manufacturing. In: *3D Printing of Pharmaceuticals*, 41–54. Springer.
[66] Vock, S., Klöden, B., Kirchner, A. et al. (2019). Powders for powder bed fusion: a review. *Progress in Additive Manufacturing* **4** (4): 383–397. https://doi.org/10.1007/s40964-019-00078-6.
[67] Mullarney, M.P., Beach, L.E., Davé, R.N. et al. (2011). Applying dry powder coatings to pharmaceutical powders using a comil for improving powder flow and bulk density. *Powder Technology* **212** (3): 397–402.
[68] Schulze, D. (2008). *Powders and Bulk Solids. Behaviour, Characterization, Storage and Flow*, **22**. Springer.
[69] Pohlman, N.A., Roberts, J.A., and Gonser, M.J. (2012). Characterization of titanium powder: microscopic views and macroscopic flow. *Powder Technology* **228**: 141–148.
[70] Fu, X., Huck, D., Makein, L. et al. (2012). Effect of particle shape and size on flow properties of lactose powders. *Particuology* **10** (2): 203–208.

[71] Ziegelmeier, S., Christou, P., Wöllecke, F. et al. (2015). An experimental study into the effects of bulk and flow behaviour of laser sintering polymer powders on resulting part properties. *Journal of Materials Processing Technology* **215**: 239–250. https://doi.org/10.1016/j.jmatprotec.2014.07.029.
[72] Schwedes, J. (2003). Review on testers for measuring flow properties of bulk solids. *Granular Matter* **5** (1): 1–43.
[73] Mohamed, E.M., Barakh Ali, S.F., Rahman, Z. et al. (2020). Formulation optimization of selective laser sintering 3D-printed tablets of clindamycin palmitate hydrochloride by response surface methodology. *AAPS Pharmscitech* **21** (6): 1–15.
[74] Vehring, R. (2008). Pharmaceutical particle engineering via spray drying. *Pharmaceutical Research* **25** (5): 999–1022.
[75] Maa, Y.-F., Costantino, H.R., Nguyen, P.-A., and Hsu, C.C. (1997). The effect of operating and formulation variables on the morphology of spray-dried protein particles. *Pharmaceutical Development and Technology* **2** (3): 213–223.
[76] Awad, A., Fina, F., Trenfield, S.J. et al. (2019). 3D printed pellets (miniprintlets): a novel, multi-drug, controlled release platform technology. *Pharmaceutics* **11** (4): 148.
[77] Sen, K., Mehta, T., Sansare, S. et al. (2021). Pharmaceutical applications of powder-based binder jet 3D printing process: a review. *Advanced Drug Delivery Reviews* **177**: 113943. https://doi.org/10.1016/j.addr.2021.113943.
[78] Sen, K., Mukherjee, R., Sansare, S. et al. (2021). Impact of powder-binder interactions on 3D printability of pharmaceutical tablets using drop test methodology. *European Journal of Pharmaceutical Sciences* **160**: 105755. https://doi.org/10.1016/j.ejps.2021.105755.
[79] Wang, -C.-C., Tejwani, M.R., Roach, W.J. et al. (2006). Development of near zero-order release dosage forms using three-dimensional printing (3-DP™) technology. *Drug Development and Industrial Pharmacy* **32** (3): 367–376.
[80] Kozakiewicz-Latała, M., Nartowski, K.P., Dominik, A. et al. (2022). Binder jetting 3D printing of challenging medicines: from low dose tablets to hydrophobic molecules. *European Journal of Pharmaceutics and Biopharmaceutics* **170**: 144–159. https://doi.org/10.1016/j.ejpb.2021.11.001.
[81] Low, K.H., Leong, K.F., Chua, C.K. et al. (2001). Characterization of SLS parts for drug delivery devices. *Rapid Prototyping Journal* **7** (5): 262–268.
[82] Leong, K.F., Chua, C.K., and Gui, W.S. (2006). Building porous biopolymeric microstructures for controlled drug delivery devices using selective laser sintering. *The International Journal of Advanced Manufacturing Technology* **31** (5): 483–489.
[83] Fina, F., Madla, C.M., Goyanes, A. et al. (2018). Fabricating 3D printed orally disintegrating printlets using selective laser sintering. *International Journal of Pharmaceutics* **541** (1–2): 101–107.
[84] Fina, F., Goyanes, A., Gaisford, S., and Basit, A.W. (2017). Selective laser sintering (SLS) 3D printing of medicines. *International Journal of Pharmaceutics* **529** (1–2): 285–293.
[85] Salmoria, G.V., Cardenuto, M.R., Roesler, C.R.M. et al. (2016). PCL/ibuprofen implants fabricated by selective laser sintering for orbital repair. *Procedia CIRP* **49**: 188–192.
[86] Salmoria, G.V., Klauss, P., Zepon, K. et al. (2012). Development of functionally-graded reservoir of PCL/PG by selective laser sintering for drug delivery devices: this paper presents a selective laser sintering-fabricated drug delivery system that contains graded progesterone content. *Virtual and Physical Prototyping* **7** (2): 107–115.
[87] Yu, D.-G., Shen, X.-X., Branford-White, C. et al. (2009). Novel oral fast-disintegrating drug delivery devices with predefined inner structure fabricated by three-dimensional printing. *Journal of Pharmacy and Pharmacology* **61** (3): 323–329.
[88] Tian, P., Yang, F., Xu, Y. et al. (2018). Oral disintegrating patient-tailored tablets of warfarin sodium produced by 3D printing. *Drug Development and Industrial Pharmacy* **44** (12): 1918–1923.
[89] Gbureck, U., Vorndran, E., Müller, F.A., and Barralet, J.E. (2007). Low temperature direct 3D printed bioceramics and biocomposites as drug release matrices. *Journal of Controlled Release* **122** (2): 173–180.
[90] Salmoria, G.V., Vieira, F.E., Muenz, E.A. et al. (2018). Additive manufacturing of PE/fluorouracil/progesterone intrauterine device for endometrial and ovarian cancer treatments. *Polymer Testing* **71**: 312–317.

[91] Hull, C.W. (1986). Apparatus for production of three-dimensional objects by stereolithography. In: US patent, Editor. US 1986.
[92] Xu, X., Awad, A., Robles-Martinez, P. et al. (2021). Vat photopolymerization 3D printing for advanced drug delivery and medical device applications. *Journal of Controlled Release* **329**: 743–757.
[93] Geever, T., Killion, J., Grehan, L. et al. (2014). Effect of photoinitiator concentration on the properties of polyethylene glycol based hydrogels for potential regenerative medicine applications. *Advances in Environmental Biology* **8**: 7–17.
[94] McDermott, S., Walsh, J.E., and Howard, R.G. (2005). A novel application of UV-LEDs in the contact lens manufacturing process. *International Society for Optics and Photonics* **5826**: 119–130.
[95] Юкатан (2015). Process of photopolymerisation. In: scheme 1 P-p, Editor 2015.
[96] Guillaume, O., Geven, M.A., Sprecher, C.M. et al. (2017). Surface-enrichment with hydroxyapatite nanoparticles in stereolithography-fabricated composite polymer scaffolds promotes bone repair. *Acta biomaterialia* **54**: 386–398.
[97] Economidou, S.N., Pere, C.P.P., Reid, A. et al. (2019). 3D printed microneedle patches using stereolithography (SLA) for intradermal insulin delivery. *Materials Science and Engineering: C* **102**: 743–755. https://doi.org/10.1016/j.msec.2019.04.063.
[98] Uddin, M.J., Scoutaris, N., Economidou, S.N. et al. (2020). 3D printed microneedles for anticancer therapy of skin tumours. *Materials Science and Engineering: C* **107**: 110248. https://doi.org/10.1016/j.msec.2019.110248.
[99] Healy, A.V., Fuenmayor, E., Doran, P. et al. (2019). Additive manufacturing of personalized pharmaceutical dosage forms via stereolithography. *Pharmaceutics* **11** (12). https://doi.org/10.3390/pharmaceutics11120645.
[100] Wang, J., Goyanes, A., Gaisford, S., and Basit, A.W. (2016). Stereolithographic (SLA) 3D printing of oral modified-release dosage forms. *International Journal of Pharmaceutics* **503** (1–2): 207–212.
[101] Goyanes, A., Det-Amornrat, U., Wang, J. et al. (2016). 3D scanning and 3D printing as innovative technologies for fabricating personalized topical drug delivery systems. *Journal of Controlled Release* **234**: 41–48.
[102] Gittard, S.D., Ovsianikov, A., Akar, H. et al. (2010). Two photon polymerization-micromolding of polyethylene glycol-gentamicin sulfate microneedles. *Advanced Engineering Materials* **12** (4): B77–B82.
[103] Melchels, F.P.W., Feijen, J., and Grijpma, D.W. (2010). A review on stereolithography and its applications in biomedical engineering. *Biomaterials* **31** (24): 6121–6130.
[104] Martinez, P.R., Goyanes, A., Basit, A.W., and Gaisford, S. (2017). Fabrication of drug-loaded hydrogels with stereolithographic 3D printing. *International Journal of Pharmaceutics* **532** (1): 313–317. https://doi.org/10.1016/j.ijpharm.2017.09.003.
[105] Vehse, M., Petersen, S., Sternberg, K. et al. (2017). Drug delivery from poly(ethylene glycol) diacrylate scaffolds produced by DLC-based micro-stereolithography. *International Journal of Pharmaceutics* **519** (1–2): 186–197.
[106] Steinbach, M., Gartz, M., and Hirsch, R. (2020). Design and characterization of 3D printable photopolymer resin containing poly(2-hydroxyethyl methacrylate) for controlled drug release. *Journal of Drug Delivery Science and Technology* **59**: 101850. https://doi.org/10.1016/j.jddst.2020.101850.
[107] Xu, X., Goyanes, A., Trenfield, S.J. et al. (2021). Stereolithography (SLA) 3D printing of a bladder device for intravesical drug delivery. *Materials Science and Engineering: C* **120**: 111773. https://doi.org/10.1016/j.msec.2020.111773.
[108] Flory, P.J. (1953). *Principles of Polymer Chemistry*. Cornell University Press.
[109] Usp, C. (2008). The United States Pharmacopeia. *National Formulary* **14**.
[110] European Pharmacopoeia (2010). European Directorate for the Quality of, and Healthcare. *European Pharmacopoeia* **1**: 2010: Council of Europe.
[111] Goyanes, A., Martinez, P.R., Buanz, A. et al. (2015). Effect of geometry on drug release from 3D printed tablets. *International Journal of Pharmaceutics* **494** (2): 657–663.

[112] Holland, B.J. and Hay, J.N. (2001). The thermal degradation of poly(vinyl alcohol). *Polymer* **42** (16): 6775–6783. https://doi.org/10.1016/S0032-3861(01)00166-5.

[113] Goyanes, A., Kobayashi, M., Martínez-Pacheco, R. et al. (2016). Fused-filament 3D printing of drug products: microstructure analysis and drug release characteristics of PVA-based caplets. *International Journal of Pharmaceutics* **514** (1): 290–295.

[114] El Aita, I., Breitkreutz, J., and Quodbach, J. (2019). On-demand manufacturing of immediate release levetiracetam tablets using pressure-assisted microsyringe printing. *European Journal of Pharmaceutics and Biopharmaceutics* **134**: 29–36.

[115] Zhang, J., Allardyce, B.J., Rajkhowa, R. et al. (2021). 3D printing of silk powder by Binder Jetting technique. *Additive Manufacturing* **38**: 101820. https://doi.org/10.1016/j.addma.2020.101820.

[116] LaFountaine, J.S., McGinity, J.W., and Williams, R.O. (2016). Challenges and strategies in thermal processing of amorphous solid dispersions: a review. *AAPS PharmSciTech* **17** (1): 43–55.

[117] Bruce, L.D., Shah, N.H., Waseem Malick, A. et al. (2005). Properties of hot-melt extruded tablet formulations for the colonic delivery of 5-aminosalicylic acid. *European Journal of Pharmaceutics and Biopharmaceutics* **59** (1): 85–97. https://doi.org/10.1016/j.ejpb.2004.06.007.

[118] Alhijjaj, M., Belton, P., and Qi, S. (2016). An investigation into the use of polymer blends to improve the printability of and regulate drug release from pharmaceutical solid dispersions prepared via fused deposition modeling (FDM) 3D printing. *European Journal of Pharmaceutics and Biopharmaceutics* **108**: 111–125. https://doi.org/10.1016/j.ejpb.2016.08.016.

[119] Parikh, T., Gupta, S.S., Meena, A., and Serajuddin, A.T.M. (2016). Investigation of thermal and viscoelastic properties of polymers relevant to hot melt extrusion-III: polymethacrylates and polymethacrylic acid based polymers. *Journal of Excipients and Food Chemicals* **5** (1): 1003.

[120] Lin, S.Y. and Yu, H.L. (1999). Thermal stability of methacrylic acid copolymers of Eudragits L, S, and L30D and the acrylic acid polymer of carbopol. *Journal of Polymer Science Part A: Polymer Chemistry* **37** (13): 2061–2067.

[121] Verma, P., Gupta, R.N., Jha, A.K., and Pandey, R. (2013). Development, *in vitro* and *in vivo* characterization of Eudragit RL 100 nanoparticles for improved ocular bioavailability of acetazolamide. *Drug Delivery* **20** (7): 269–276.

[122] Diarra, M., Pourroy, G., Boymond, C., and Muster, D. (2003). Fluoride controlled release tablets for intrabuccal use. *Biomaterials* **24** (7): 1293–1300.

[123] Hao, S., Wang, B., Wang, Y. et al. (2013). Preparation of Eudragit L 100-55 enteric nanoparticles by a novel emulsion diffusion method. *Colloids and Surfaces B: Biointerfaces* **108**: 127–133.

[124] Quinteros, D.A., Manzo, R.H., and Allemandi, D.A. (2010). Design of a colonic delivery system based on cationic polymethacrylate (Eudragit E100)-mesalamine complexes. *Drug Delivery* **17** (4): 208–213.

[125] Yoo, J.-W., Giri, N., and Lee, C.H. (2011). pH-sensitive Eudragit nanoparticles for mucosal drug delivery. *International Journal of Pharmaceutics* **403** (1–2): 262–267.

[126] Verma, P.R.P. and Iyer, S.S. (2000). Transdermal delivery of propranolol using mixed grades of Eudragit: design and *in vitro* and *in vivo* evaluation. *Drug Development and Industrial Pharmacy* **26** (4): 471–476.

[127] Katstra, W.E., Palazzolo, R.D., Rowe, C.W. et al. (2000). Oral dosage forms fabricated by three dimensional printing™. *Journal of Controlled Release* **66** (1): 1–9.

[128] Rowe, C., Katstra, W., Palazzolo, R. et al. (2000). Multimechanism oral dosage forms fabricated by three dimensional printing™. *Journal of Controlled Release* **66** (1): 11–17.

[129] Holländer, J., Genina, N., Jukarainen, H. et al. (2016). Three-dimensional printed PCL-based implantable prototypes of medical devices for controlled drug delivery. *Journal of Pharmaceutical Sciences* **105** (9): 2665–2676. https://doi.org/10.1016/j.xphs.2015.12.012.

[130] Gunatillake, P., Mayadunne, R., and Adhikari, R. (2006). Recent developments in biodegradable synthetic polymers. *Biotechnology Annual Review* **12**: 301–347.

[131] Wang, K.A.-O. and Deng, Q.A.-O. (2019). The thermal and mechanical properties of poly(ethylene-co-vinyl acetate) random copolymers (PEVA) and its covalently crosslinked analogues. *Polymers* **11** (6): 1055.

[132] Vrandečić, N., Erceg, M., Jakić, M., and Klarić, I. (2010). Kinetic analysis of thermal degradation of poly(ethylene glycol) and poly(ethylene oxide)s of different molecular weight. *Thermochimica Acta* **498**: 71–80. https://doi.org/10.1016/j.tca.2009.10.005.

[133] Stewart, S.A., Domínguez-Robles, J., McIlorum, V.J. et al. (2020). Development of a biodegradable subcutaneous implant for prolonged drug delivery using 3D printing. *Pharmaceutics* **12** (2). https://doi.org/10.3390/pharmaceutics12020105.

[134] Gilding, D.K. and Reed, A.M. (1979). Biodegradable polymers for use in surgery: polyglycolic/poly(actic acid) homo- and copolymers: 1. *Polymer* **20** (12): 1459–1464. https://doi.org/10.1016/0032-3861(79)90009-0.

[135] Ulery, B.D., Nair, L.S., and Laurencin, C.T. (2011). Biomedical applications of biodegradable polymers. *Journal of Polymer Science Part B: Polymer Physics* **49** (12): 832–864. https://doi.org/10.1002/polb.22259.

[136] Wang, G. and Li, A. (2008). Thermal decomposition and kinetics of mixtures of polylactic acid and biomass during copyrolysis. *Chinese Journal of Chemical Engineering* **16** (6): 929–933. https://doi.org/10.1016/S1004-9541(09)60018-5.

[137] Samantaray, P.K., Little, A., Haddleton, D.M. et al. (2020). Poly(glycolic acid) (PGA): a versatile building block expanding high performance and sustainable bioplastic applications. *Green Chemistry* **22** (13): 4055–4081. https://doi.org/10.1039/D0GC01394C.

[138] Seoane-Viaño, I., Gómez-Lado, N., Lázare-Iglesias, H. et al. (2020). 3D printed tacrolimus rectal formulations ameliorate colitis in an experimental animal model of inflammatory bowel disease. *Biomedicines* **8** (12). https://doi.org/10.3390/biomedicines8120563.

[139] Zhang, J., Feng, X., Patil, H. et al. (2017). Coupling 3D printing with hot-melt extrusion to produce controlled-release tablets. *International Journal of Pharmaceutics* **519** (1): 186–197. https://doi.org/10.1016/j.ijpharm.2016.12.049.

[140] Yang, Y., Wang, H., Xu, X., and Yang, G. (2021). Strategies and mechanisms to improve the printability of pharmaceutical polymers Eudragit® EPO and Soluplus®. *International Journal of Pharmaceutics* **599**: 120410.

[141] Azad, M.A., Olawuni, D., Kimbell, G. et al. (2020). Polymers for extrusion-based 3D printing of pharmaceuticals: a holistic materials–process perspective. *Pharmaceutics* **12** (2): 124.

[142] Fisher, J.P., Dean, D., and Mikos, A.G. (2002). Photocrosslinking characteristics and mechanical properties of diethyl fumarate/poly(propylene fumarate) biomaterials. *Biomaterials* **23** (22): 4333–4343. https://doi.org/10.1016/S0142-9612(02)00178-3.

[143] Zhou, W., Qiao, Z., Nazarzadeh Zare, E. et al. (2020). 4D-printed dynamic materials in biomedical applications: chemistry, challenges, and their future perspectives in the clinical sector. *Journal of Medicinal Chemistry* **63** (15): 8003–8024.

[144] Brady, J., Dürig, T., Lee, P.I., and Li, J.X. (2017). Polymer properties and characterization. In: *Developing Solid Oral Dosage Forms*, 181–223. Elsevier.

[145] Zema, L., Loreti, G., Melocchi, A. et al. (2013). Gastroresistant capsular device prepared by injection molding. *International Journal of Pharmaceutics* **440** (2): 264–272.

[146] Thakkar, R., Thakkar, R., Pillai, A. et al. (2020). Systematic screening of pharmaceutical polymers for hot melt extrusion processing: a comprehensive review. *International Journal of Pharmaceutics* **576**: 118989.

[147] Chai, X., Chai, H., Wang, X. et al. (2017). Fused deposition modeling (FDM) 3D printed tablets for intragastric floating delivery of domperidone. *Scientific Reports* **7** (1): 1–9.

[148] Gómez-Carracedo, A., Alvarez-Lorenzo, C., Gómez-Amoza, J.L., and Concheiro, A. (2003). Chemical structure and glass transition temperature of non-ionic cellulose ethers. *Journal of Thermal Analysis and Calorimetry* **73** (2): 587–596.

[149] Chavan, R.B., Rathi, S., Vgss, J., and Shastri, N.R. (2019). Cellulose based polymers in development of amorphous solid dispersions. *Asian Journal of Pharmaceutical Sciences* **14** (3): 248–264.

[150] Michailidou, G., Terzopoulou, Z., Kehagia, A. et al. (2021). Preliminary evaluation of 3D printed chitosan/pectin constructs for biomedical applications. *Marine Drugs* **19** (1): 36.
[151] Farrugia, C.A. and Groves, M.J. (1999). Gelatin behaviour in dilute aqueous solution: designing a nanoparticulate formulation. *Journal of Pharmacy and Pharmacology* **51** (6): 643–649.
[152] Inzana, J.A., Olvera, D., Fuller, S.M. et al. (2014). 3D printing of composite calcium phosphate and collagen scaffolds for bone regeneration. *Biomaterials* **35** (13): 4026–4034.
[153] Billiet, T., Gevaert, E., De Schryver, T. et al. (2014). The 3D printing of gelatin methacrylamide cell-laden tissue-engineered constructs with high cell viability. *Biomaterials* **35** (1): 49–62.
[154] Porter, C.J.H., Trevaskis, N.L., and Charman, W.N. (2007). Lipids and lipid-based formulations: optimizing the oral delivery of lipophilic drugs. *Nature Reviews Drug Discovery* **6** (3): 231–248.
[155] Vithani, K., Hawley, A., Jannin, V. et al. (2017). Inclusion of digestible surfactants in solid SMEDDS formulation removes lag time and influences the formation of structured particles during digestion. *AAPS Journal* **19**: 754–764.
[156] Pouton, C.W. (2000). Lipid formulations for oral administration of drugs: non-emulsifying, self-emulsifying and 'self-microemulsifying' drug delivery systems. *European Journal of Pharmaceutical Sciences* **11**: S93–S98.
[157] Kang, B.K., Lee, J.S., Chon, S.K. et al. (2004). Development of self-microemulsifying drug delivery systems (SMEDDS) for oral bioavailability enhancement of simvastatin in Beagle dogs. *International Journal of Pharmaceutics* **274** (1–2): 65–73.
[158] Vithani, K., Goyanes, A., Jannin, V. et al. (2019). A proof of concept for 3D printing of solid lipid-based formulations of poorly water-soluble drugs to control formulation dispersion kinetics. *Pharmaceutical Research* **36** (7): 102. https://doi.org/10.1007/s11095-019-2639-y.
[159] Karavasili, C., Gkaragkounis, A., Moschakis, T. et al. (2020). Pediatric-friendly chocolate-based dosage forms for the oral administration of both hydrophilic and lipophilic drugs fabricated with extrusion-based 3D printing. *European Journal of Pharmaceutical Sciences* **147**: 105291. https://doi.org/10.1016/j.ejps.2020.105291.
[160] Seoane-Viaño, I., Ong, J.J., Luzardo-Álvarez, A. et al. (2021). 3D printed tacrolimus suppositories for the treatment of ulcerative colitis. *Asian Journal of Pharmaceutical Sciences* **16** (1): 110–119.
[161] Kyobula, M., Adedeji, A., Alexander, M.R. et al. (2017). 3D inkjet printing of tablets exploiting bespoke complex geometries for controlled and tuneable drug release. *Journal of Controlled Release* **261**: 207–215. https://doi.org/10.1016/j.jconrel.2017.06.025.
[162] Okwuosa, T.C., Pereira, B.C., Arafat, B. et al. (2017). Fabricating a shell-core delayed release tablet using dual FDM 3D printing for patient-centred therapy. *Pharmaceutical Research* **34** (2): 427–437.
[163] Melocchi, A., Uboldi, M., Inverardi, N. et al. (2019). Expandable drug delivery system for gastric retention based on shape memory polymers: development via 4D printing and extrusion. *International Journal of Pharmaceutics* **571**: 118700. https://doi.org/10.1016/j.ijpharm.2019.118700.
[164] Palekar, S., Nukala, P.K., Mishra, S.M. et al. (2019). Application of 3D printing technology and quality by design approach for development of age-appropriate pediatric formulation of baclofen. *International Journal of Pharmaceutics* **556**: 106–116. https://doi.org/10.1016/j.ijpharm.2018.11.062.
[165] Ilyés, K., Kovács, N.K., Balogh, A. et al. (2019). The applicability of pharmaceutical polymeric blends for the fused deposition modelling (FDM) 3D technique: material considerations–printability–process modulation, with consecutive effects on *in vitro* release, stability and degradation. *European Journal of Pharmaceutical Sciences* **129**: 110–123. https://doi.org/10.1016/j.ejps.2018.12.019.
[166] Prasad, E., Islam, M.T., Goodwin, D.J. et al. (2019). Development of a hot-melt extrusion (HME) process to produce drug loaded Affinisol™ 15LV filaments for fused filament fabrication (FFF) 3D printing. *Additive Manufacturing* **29**: 100776.

[167] Sadia, M., Sośnicka, A., Arafat, B. et al. (2016). Adaptation of pharmaceutical excipients to FDM 3D printing for the fabrication of patient-tailored immediate release tablets. *International Journal of Pharmaceutics* **513** (1–2): 659–668.

[168] Ehtezazi, T., Algellay, M., Islam, Y. et al. (2018). The application of 3D printing in the formulation of multilayered fast dissolving oral films. *Journal of Pharmaceutical Sciences* **107** (4): 1076–1085.

[169] Saviano, M., Aquino, R.P., Del Gaudio, P. et al. (2019). Poly(vinyl alcohol) 3D printed tablets: the effect of polymer particle size on drug loading and process efficiency. *International Journal of Pharmaceutics* **561**: 1–8. https://doi.org/10.1016/j.ijpharm.2019.02.025.

[170] Goyanes, A., Fernández-Ferreiro, A., Majeed, A. et al. (2018). PET/CT imaging of 3D printed devices in the gastrointestinal tract of rodents. *International Journal of Pharmaceutics* **536** (1): 158–164.

[171] Gioumouxouzis, C.I., Baklavaridis, A., Katsamenis, O.L. et al. (2018). A 3D printed bilayer oral solid dosage form combining metformin for prolonged and glimepiride for immediate drug delivery. *European Journal of Pharmaceutical Sciences* **120**: 40–52.

[172] Zhang, J., Yang, W., Vo, A.Q. et al. (2017). Hydroxypropyl methylcellulose-based controlled release dosage by melt extrusion and 3D printing: structure and drug release correlation. *Carbohydrate Polymers* **177**: 49–57.

[173] Kimura, S-i., Ishikawa, T., Iwao, Y. et al. (2019). Fabrication of zero-order sustained-release floating tablets via fused depositing modeling 3D printer. *Chemical and Pharmaceutical Bulletin* **67** (9): 992–999.

[174] Drašković, M., Medarević, D., Aleksić, I., and Parojčić, J. (2017). *In vitro* and *in vivo* investigation of taste-masking effectiveness of Eudragit E PO as drug particle coating agent in orally disintegrating tablets. *Drug Development and Industrial Pharmacy* **43** (5): 723–731.

[175] Goyanes, A., Scarpa, M., Kamlow, M. et al. (2017). Patient acceptability of 3D printed medicines. *International Journal of Pharmaceutics* **530** (1): 71–78. https://doi.org/10.1016/j.ijpharm.2017.07.064.